



Relation between the helical twist and S-shaped cross section of the lamellar crystals of polyethylene

Takayuki Ikehara & Toshiyuki Kataoka

Department of Material and Life Chemistry, Faculty of Engineering, Kanagawa University, 3-27-1, Rokkakubashi, Kanagawa-ku, Yokohama, 221-8686, Japan.

SUBJECT AREAS:

STRUCTURE OF SOLIDS
AND LIQUIDS

CHEMICAL PHYSICS

APPLIED PHYSICS

POLYMER CHARACTERIZATION

Received

23 November 2012

Accepted

26 February 2013

Published

13 March 2013

Correspondence and
requests for materials
should be addressed to

T.I. (ikehara@
kanagawa-u.ac.jp)

The relation between the handedness of helical twist and the S-shaped cross section of the lamellar crystals is discussed for linear polyethylene. The lamellar crystals are found to rotate so that the convex surfaces of “S” push aside the melt when they advance in the growth direction. This relation, which has not been examined sufficiently so far, is found to be opposite from what was proposed earlier. A model to explain these observations is presented. This paper also demonstrates that the twist handedness can be clarified based on the stack order of crystalline lamellae without any treatment such as etching or extraction to isolate the lamellar crystals.

Helices and chirality are extensively investigated in various research fields^{1–4}. With regard to polymeric substances, not only chirality in the chain conformations⁴, but helices of lamellar crystals have also attracted researchers’ interests as described below.

Crystalline polymers often exhibit banded spherulites with regular concentric extinction rings when they are observed by polarized optical microscopy. The origin is ascribed to the twist of lamellar crystals, or simply called lamellae, that grow in the radial direction from the centre of spherulites^{5–11}. Studies using electron and atomic force microscopy^{12–19} and x-ray diffraction⁸ provided the evidence for the twisted structures. Two models have been proposed to explain the lamellar twist: one is based on the surface stress of the lamellar crystals^{9,10,20} and the other is based on the consecutive formation of screw dislocations on the lamellae^{21,22}. Hereafter, the twists formed through the former and latter models are addressed as continuous and dislocation types, respectively. The twist pitches are discussed based on the lamellar thickness⁹ and the field gradient²³. A review on the lamellar twist is also published²⁴.

Twisted lamellae are also reported to have an S-shaped cross section when they are cut perpendicularly to the growth direction^{10,25–27}. This structure is explained based on the reorientation of polymer chains and the stress on the lamellar surfaces¹⁰, and self-induced fields during crystallization¹¹. The relation between the twist sense, namely left- or right-handed rotation, and the curvature of the S-profile for the continuous type was proposed that the concave surfaces of an S scoop up the melt when lamellar crystals grow^{25,26}. On the other hand, for the dislocation type²¹, which are formed at relatively high crystallization temperatures, the relation between the senses of twist and S are opposite²²; the convex surfaces push aside the melt.

Nevertheless, only a few works that contain discussion on the relation between the twist and the S-profile are found^{10,11,22}. The experimental examination of the relation for the continuously twisted lamellae is still insufficient although that for the dislocation type was discussed based on clear electron micrographs²².

With these respects, the relation of the S-shaped lamellar profile with the twist handedness is examined and discussed in this paper for polyethylene, whose crystallization behaviour has been investigated extensively thus far, including the formation of banded spherulites. For this purpose, the twisted structure of lamellar stacks is investigated by atomic force microscopy (AFM) to obtain the twist handedness and the lamellar profile. This paper also demonstrates that the twist sense can be clarified based on the stack order of lamellae without any treatment such as etching or extraction, which have often been employed in many works by microscopy to observe clearer structures.

Results

Figure 1 shows the polarized optical micrograph of the banded spherulites of the sample. It shows that the band spacing of the spherulites grown at 118°C is about 1.8 μm.

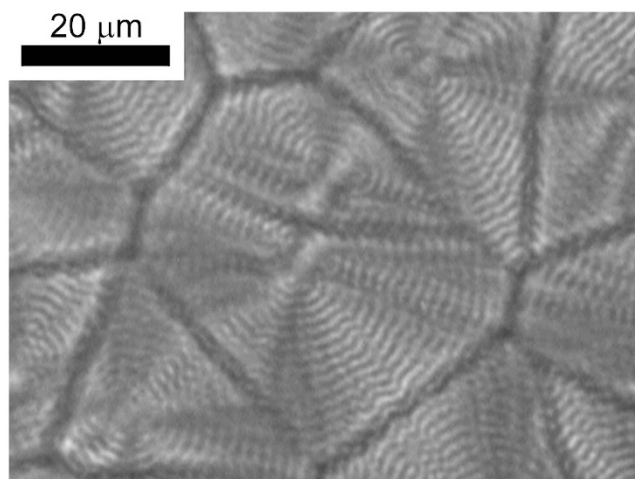


Figure 1 | Polarized optical micrograph of banded spherulites of polyethylene. The crystallization temperature is 118°C.

The results of the AFM observation are displayed in Figure 2. Here, four images were connected to each other to obtain clearer structures in a broad area. The lamellar growth direction is from the left to the right. The topographic image in Figure 2(a) shows a periodic rugged surface that represents the banded structure. The lamellae are placed edge-on and flat-on against the substrate in the higher and lower parts, respectively. The amplitude-error image in Figure 2(b), on the other hand, emphasizes the edges of uneven surfaces. The arrows A and B on top of the picture indicate the edge-on and flat-on parts, respectively.

The lamellar stacks on the left- and right-hand sides of the edge-on parts (e.g. arrows C and D, respectively) show different superposition orders. In part C, a lamella that is closer to the top of the picture covers another lamella that is closer to the bottom of the picture. In part D, the stack order is opposite; a lamella that is closer to the bottom of the picture covers another one that is closer to the top of the picture. This situation is the same for the stacks E–F and G–H. The three-dimensional representation in Figure 2(c), which is based on the height image of Figure 2(a) around the stack C–D, also indicates the lamellar twist and the inversion of the stack order.

These observations indicate the twist of lamellae as schematically illustrated in Figure 3. The order of the lamellar stacks inverts when the lamellae change their alignment from flat-on to edge-on and back to flat-on. The rotational sense is left-handed regarding the growth direction in the present case.

The growth of the lamellae on the surface stopped in the flat-on regions as indicated by the arrow K of Figure 2(b). This is probably ascribed to the depletion of the crystallizing polymer on the surface. The two diagonal facets against the growth direction should be the 110 surfaces since the growth direction of polyethylene is toward the *b*-axis. The lamellae in the flat-on parts are not as twisted as in the edge-on parts. The topography in Figure 2(a) also indicates little change in the tilt angle concerning the growth direction.

The stack orders on the left- and right-hand sides of the flat-on parts are also different (e.g. arrows J and E, respectively). This can be explained if the continuous lamellar twist is assumed to be underneath the top layers of the terminated growth lamellae in the flat-on parts.

The cross-sectional profile of the edge-on lamellae looks rounded, especially around the arrows C, E, and G in Figure 2(b). The convex and concave surfaces are faced to the top and the bottom of the picture, respectively. The lamellae at D and also those above the letter “K” exhibit concave surfaces. Figure 2(c) also indicates the convex and concave surfaces at C and D, respectively. The lamellar profiles at these places must be the upper halves of the S-shaped profile^{10,25–27},

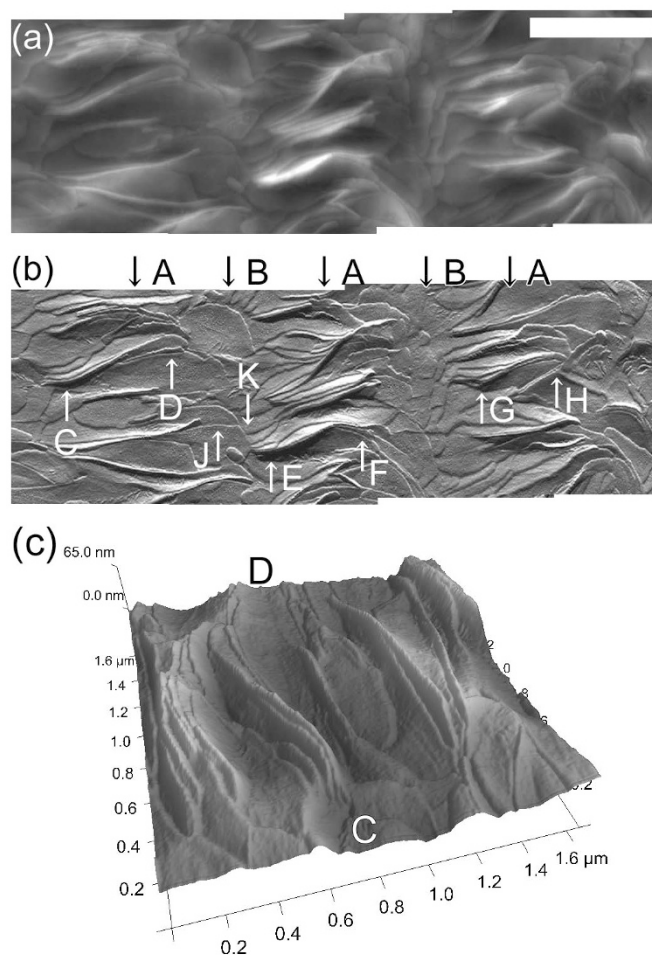


Figure 2 | AFM images of banded structures of polyethylene: (a) topographic and (b) amplitude-error images. The three-dimensional representation of the topography around C–D is exhibited in (c). The scale bar in the upper right corner of (a) indicates 1 μm. The scale of (b) is the same as that of (a). The grey scale from black to white is 100 nm in (a). The lamellar growth direction is from the left to the right for (a) and (b).

although the other halves are underneath the surface and the profile cannot fully be confirmed by AFM. On the other hand, the AFM images also indicated almost planar lamellae such as those underneath the arrow J. The growth of these planar lamellae is terminated in the flat-on regions. The profiles of the continuously twisting lamellae underneath them are unknown from the present data.

The present observations showed that the lamellae rotate in regard to the growth direction so that the convex faces of the “S” push aside

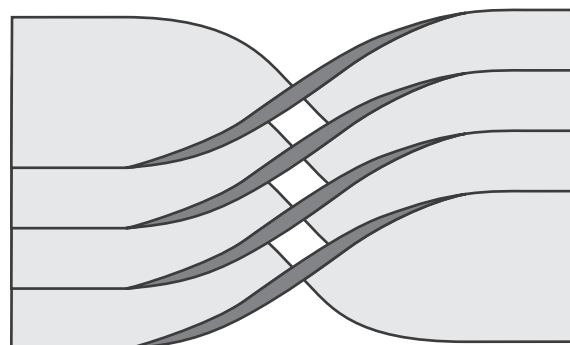


Figure 3 | Schematic figure of a twisted lamellar stack, where the superposition order of lamellae inverts when they twist.

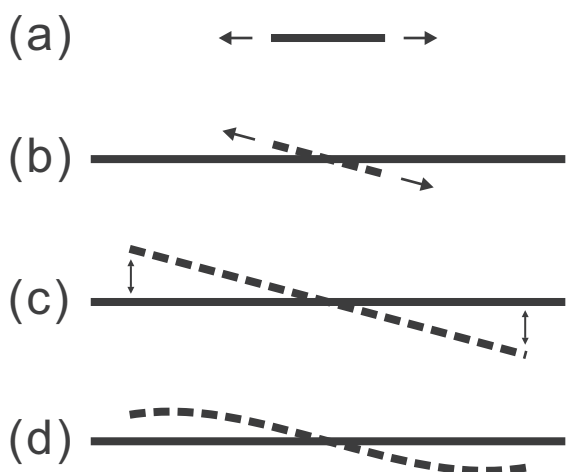


Figure 4 | Schematic figure of the cross sections of lamellae. (a) The tip of a flat-on lamella, (b) laterally grown flat-on lamella (solid line) and the tip of the twisted lamella (dashed line), (c) laterally grown twisted lamella (dashed line), and (d) the formation of the S profile. The arrows indicate the lateral growth of lamellae, and the lamellar growth direction is toward the reader.

the melt. The relation between the rotational sense and the S-shaped profile in the present work is different from what was reported earlier^{25,26}, where the lamellae were proposed to twist so that the concave surfaces scoop up the melt. The present relation is for the dislocation type²². However, no screw dislocation was found in the present results. The lamellae showed smooth edges with no clear indications of the consecutive formation of screw dislocations, which are formed on the edges of lamellae as indicated in the figures in the literature^{21,23}. If the observed twist was that of the dislocation type, the dislocations would make the lamellar edges discontinuous.

Discussion

The present results on the twist handedness and the S-shaped profile enable us to discuss the relation between them. The followings can be a possible explanation for the observed relation. Figure 4(a) shows a cross section close to the growth tip of a lamella in a flat-on region. Here, the initial lamellar profile is assumed to be almost planar. The width of the lamellar tips is still small as indicated by the arrow K of Figure 2(b). The lamellar growth direction is toward the reader and it also grows laterally as indicated by the arrows. In Figure 4(b), the lamella has grown for some distance toward the reader. The dashed line indicates the cross section close to the growth tip, as in Figure 4(a). It is a little twisted against the cross section at the solid line, which has a sufficient lateral width at this moment. The profile at the dashed line should be almost planar since the central part of an “S” has little curvature and the lamellar width is still narrow enough. The lamella at the dashed line also grows laterally as indicated by the arrows. The cross sections at the dashed and the solid lines are connected by a continuous lamella. Both edges of the dashed cross section are exerted to a tension between the solid and dashed cross sections as in Figure 4(c). The lamella has to bend itself to release the tension as indicated by Figure 4(d), where the profile is S-shaped. The sense of lamellar twist and the S-shaped profile formed in this way are identical with the present observations.

The model described here should contribute to determining the relation between the twist handedness and the sense of the S-profile when the tip of a lamella is twisted. Then, other models^{10,11} may also contribute to the formation of the S-profile.

The present model can also explain the almost planar profile of the terminated lamellae in the flat-on regions (e.g. the ones underneath the arrow J in Figure 2(b)), where there is little lamellar twist. They do

not have to change their profile for a negligible twist in the flat-on region since no tension arises as explained in Figure 4(c). The lamellar profile may be an outcome of lamellar twist based on this model. The lamellae underneath these crystals should have an S-shaped profile if they are continuously twisted although the profile cannot be confirmed by AFM.

The growth direction of the crystals should also be taken into account when discussing the relation between the lamellar profile and the twist handedness. If the growth direction was opposite, the relation would be different from the present case; the lamellae would twist such that the concave faces scoop up the melt in this case. The results in Figure 2 exhibited the tapered growth tips (e.g. arrow K). The growth direction is obviously from the left- to right-hand side in Figure 2(a) and (b). The growth direction is also incorporated in the present model as described above. On the other hand, the relation with respect to the growth direction is ambiguous for the former models^{10,11}.

Methods

Linear or high density polyethylene (HDPE, $M_w = 125,000$, product number 181900) was purchased from Sigma-Aldrich Company. Branched or low density polyethylene (LDPE) used in this study was Novatec LF441B, which is a commercial high-pressure LDPE produced by Japan Polyethylene Corporation and has a wide range of branch lengths (density 0.924 g/cm^3 and melt flow ratio 2.0 g/10 min at 190°C). When blended samples of HDPE and LDPE crystallize, the uncrystallizable parts around the branch points in LDPE are expelled from the crystalline lattice, which results in wider interlamellar regions and consequently clearer lamella-stacked structures. The melting temperature ranges of HDPE and LDPE are around 130°C and 110°C , respectively, when heated at a rate of 10°C/min .

The substances were dissolved into hot xylene with the overall concentration of about 1 wt%. The weight ratio of the HDPE/LDPE blend was 8/2. The hot solution was dropped onto an optical glass plate, dried in a fume hood for two hours, and then in a vacuum for two days at 40°C . The thickness of the obtained film was about $5 \mu\text{m}$. The sample was first melted at 150°C for 3 min using a temperature-controlled stage for optical microscopy (Linkam, LK-600PM), quenched to the isothermal crystallization temperature of 118°C at a cooling rate of about 100°C/min using a nitrogen gas flow inside the heating unit. The sample was observed as is, i.e. no further treatment such as etching was applied to the sample to avoid the formation of artefacts or the collapse of structures. All morphological investigations were performed at room temperature.

Figure 1 was acquired with a polarizing optical microscope (Olympus, BX-51) and a digital camera (Roper Scientific, CoolSNAP 5.0). The original resolution was 1280×960 pixels.

Figure 2 was acquired by atomic force microscopy (Veeco, Nanoscope V) in the tapping mode with cantilevers having a spring constant of about 40 N/m and a resonant frequency of about 300 kHz (Veeco, RTESP). The resolution was 256×256 pixels. Connection of multiple data was done on Adobe Photoshop 7.0.

The annotation of the pictures in Figures 1 and 2 with characters, arrows and bars was performed on Adobe Photoshop 7.0.

- Luscher, M. Exact chiral symmetry on the lattice and the Ginsparg-Wilson relation. *Phys. Lett. B* **428**, 342–345 (1998).
- Sanna, M. G. *et al.* Enhancement of capillary leakage and restoration of lymphocyte egress by a chiral S1P(1) antagonist in vivo. *Nature Chem. Bio.* **2**, 434–441 (2006).
- Taylor, M. S. & Jacobsen, E. N. Asymmetric catalysis by chiral hydrogen-bond donors. *Angew. Chem. Int. Ed.* **45**, 1520–1543 (2006).
- Green, M. M. *et al.* The Macromolecular Route to Chiral Amplification. *Angew. Chem. Int. Ed.* **38**, 3138–3154 (1999).
- Keith, H. D. & Padden, F. J. The optical behavior of spherulites in crystalline polymers. Part II. The growth and structure of the spherulites. *J. Polym. Sci.* **39**, 123–138 (1959).
- Keller, A. Investigations on banded spherulites. *J. Polym. Sci.* **39**, 151–173 (1959).
- Price, F. P. On extinction patterns of polymer spherulites. *J. Polym. Sci.* **39**, 139–150 (1959).
- Fujiwara, Y. The superstructure of melt-crystallized polyethylene. I. Screwlike orientation of unit cell in polyethylene spherulites with periodic extinction rings. *J. Appl. Polym. Sci.* **4**, 10–15 (1960).
- Okano, K. Note on the Lamellar Twist in Polymer Spherulites. *Jpn. J. Appl. Phys.* **3**, 351–353 (1964).
- Keith, H. D. & Padden, F. J. Twisting orientation and the role of transient states in polymer crystallization. *Polymer* **25**, 28–42 (1984).
- Schultz, J. M. Self-induced field model for crystal twisting in spherulites. *Polymer* **44**, 433–441 (2003).
- Keller, A. & Sawada, S. On the interior morphology of bulk polyethylene. *Makromol. Chem.* **74**, 190–221 (1964).



13. Kunz, M., Dreschler, M. & Möller, M. On the structure of ultra-high molecular weight polyethylene gels. *Polymer* **36**, 1331–1339 (1995).
14. Li, C. *et al.* Double-Twisted Helical Lamellar Crystals in a Synthetic Main-Chain Chiral Polyester Similar to Biological Polymers. *Macromolecules* **32**, 524–527 (1999).
15. Sasaki, S., Sakaki, Y., Takahara, A. & Kajiyama, T. Microscopic lamellar organization in high-density polyethylene banded spherulites studied by scanning probe microscopy. *Polymer* **43**, 3441–3446 (2002).
16. Xu, J. *et al.* Direct AFM Observation of Crystal Twisting and Organization in Banded Spherulites of Chiral Poly(3-hydroxybutyrate-co-3-hydroxyhexanoate). *Macromolecules* **37**, 4118–4123 (2004).
17. Wang, Z. *et al.* Twisting of Lamellar Crystals in Poly(3-hydroxybutyrate-co-3-hydroxyvalerate) Ring-Banded Spherulites. *Macromolecules* **43**, 4441–4444 (2010).
18. Li, J. *et al.* Increasing Lamellar Twisting Frequency with Poly(lactic acid) Segments Incorporation in Poly(trimethylene terephthalate) Ring-Banded Spherulites. *Macromolecules* **44**, 2918–2925 (2011).
19. Liu, J., Ye, H.-M., Xu, J. & Guo, B.-H. Formation of ring-banded spherulites of a and b modifications in Poly(butylene adipate). *Polymer* **52**, 4619–4630 (2011).
20. Rosenthal, M., Bar, G., Burghammer, M. & Ivanov, D. A. On the Nature of Chirality Imparted to Achiral Polymers by the Crystallization Process. *Angew. Chem. Int. Ed.* **50**, 8881–8885 (2011).
21. Schultz, J. M. & Kinloch, D. R. Transverse screw dislocations: A source of twist in crystalline polymer ribbons. *Polymer* **10**, 271–278 (1969).
22. Toda, A. & Keller, A. Growth of polyethylene single crystals from the melt: Morphology. *Colloid. Polym. Sci.* **271**, 328–342 (1993).
23. Toda, A., Okamura, M., Taguchi, K., Hikosaka, M. & Kajioka, H. Branching and Higher Order Structure in Banded Polyethylene Spherulites. *Macromolecules* **41**, 2484–2493 (2008).
24. Lotz, B. & Cheng, S. Z. D. A critical assessment of unbalanced surface stresses as the mechanical origin of twisting and scrolling of polymer crystals. *Polymer* **46**, 577–610 (2005).
25. Bassett, D. C. & Hodge, A. M. On the Morphology of Melt-Crystallized Polyethylene I. Lamellar Profiles. *Proc. Roy. Soc. London A* **377**, 25–37 (1981).
26. Bassett, D. C. & Hodge, A. M. On the Morphology of Melt-Crystallized Polyethylene. III. Spherulitic Organization. *Proc. Roy. Soc. London A* **377**, 61–71 (1981).
27. Ikehara, T., Jinnai, H., Kaneko, T., Nishioka, H. & Nishi, T. Local Lamellar Structures in Banded Spherulites Analyzed by Three-Dimensional Electron Tomography. *J. Polym. Sci. Part B Polym. Phys.* **45**, 1122–1125 (2007).

Acknowledgements

This work was partly supported by a Grant-in-Aid for Scientific Research (C) from Japan Society for the Promotion of Science (22550201). The authors thank Mr. Syuichi Yuda for his help in the experiments.

Author contributions

T.I. designed the experiments and wrote the main manuscript text. T.K. obtained the pictures in Figures 1 and 2. All authors reviewed the manuscript.

Additional information

Competing financial interests: The authors declare no competing financial interests.

License: This work is licensed under a Creative Commons Attribution-NonCommercial-NoDerivs 3.0 Unported License. To view a copy of this license, visit <http://creativecommons.org/licenses/by-nc-nd/3.0/>

How to cite this article: Ikehara, T. & Kataoka, T. Relation between the helical twist and S-shaped cross section of the lamellar crystals of polyethylene. *Sci. Rep.* **3**, 1444; DOI:10.1038/srep01444 (2013).